

## Compatibilizing Effect of Graphite Oxide in Graphene/PMMA Nanocomposites

Jin Young Jang and Han Mo Jeong\*

Department of Chemistry, University of Ulsan, Ulsan 680-749, Korea

Byung Kyu Kim

Department of Polymer Science and Engineering, Pusan National University, Busan 609-735, Korea

Received September 22, 2008; Revised December 19, 2008;

Accepted December 20, 2008

### Introduction

The structure of single graphene sheets, which are the basal plane of graphite, can be best visualized by making a longitudinal scission on a single wall carbon nanotube (SWCNT) along the tube axis and flattening the resulting sheet.<sup>1</sup> These sheets have electric conductivity, thermal conductivity, and tensile modulus values similar to SWCNTs, and can be used as alternatives to SWCNTs in various applications.<sup>2-5</sup>

Graphite shows a sharp X-ray diffraction peak at  $2\theta=26.5^\circ$  because it has a layered structure composed of graphene sheets and the typical interlayer spacing is 3.35 Å. These sheets are one-atom-thick and are composed of hexagonal carbon rings. Graphite oxide (GO), prepared by oxidizing graphite, is a graphite-derived compound with a layered structure. GO has a broad X-ray diffraction peak at lower angles than graphite, normally  $2\theta=10\sim 15^\circ$ , because polar groups such as hydroxyl, epoxide, ether, and carboxylate groups are present on graphene sheets as a result of oxidation and expand the interlayer spacing.<sup>2,6-8</sup>

Recently, it has been reported that exfoliation of graphite into a single graphene sheet can be achieved from sufficiently oxidized GO, if inter-graphene spacing associated with native graphite is completely eliminated in the oxidation stage, and if adequate pressure builds up at the gallery between the GO sheets by rapid heating. The pressure results from CO<sub>2</sub> evolved by the thermal decomposition of functional groups.<sup>3,4,9</sup> This exfoliated graphite, where the inter-graphene spaces associated with GO and graphite are completely excluded after thermal expansion, has an affinity for polar solvents and polymers, as well as good conductivity, because this exfoliated graphite is composed of

functionalized graphene sheets (FGSs) having polar functional groups remained even after thermal treatment.<sup>3,5</sup> Normally, carbon nanotubes need surface treatment if they are to be used as a nanofiller for fine dispersion in a polymer matrix.<sup>10-13</sup> However, FGS can offer comparable or better electrical conductivity enhancement than carbon nanotubes without further surface treatment, owing to the polar functional groups.<sup>9,14</sup>

Our laboratory has prepared and examined FGS nanocomposites with various polymers.<sup>15,16</sup> During these studies, we discovered that the fine dispersion of FGS in a polymer matrix can be improved when GO is used as a compatibilizer. This paper reports the compatibilizing effect of GO in FGS/poly(methyl methacrylate) (PMMA) nanocomposites.

### Experimental

**Materials.** Natural graphite, HC-598 and HC-908 with average particle sizes of 11 and 8 μm, respectively, was purchased from Hyundai Coma Co., Ltd. Methyl methacrylate (MMA, Aldrich), 2,2'-azobisisobutyronitrile (AIBN, Aldrich), tetrahydrofuran (THF, Aldrich), concentrated H<sub>2</sub>SO<sub>4</sub> (96%, DC Chemical Co., Ltd. or Matsunoen Chemicals Co.), fuming HNO<sub>3</sub> (Matsunoen Chemicals Co.), KMnO<sub>4</sub> (Duksan Pure Chemical), KClO<sub>3</sub> (Samchun Pure Chemical Co.), H<sub>2</sub>O<sub>2</sub> (30%, DC Chemical Co., Ltd.), and hydrochloric acid (35%, Daejung Chemicals & Metals Co., Ltd.) were used as received.

**GO Preparation.** GO used as a compatibilizer (GO-1) was prepared by oxidizing graphite with KMnO<sub>4</sub>/H<sub>2</sub>SO<sub>4</sub>.<sup>15,17,18</sup> Elemental analysis showed that the GO composition was C<sub>10</sub>O<sub>2.28</sub>H<sub>1.31</sub>. The conductivity was 0.5 S/cm.

**FGS Preparation.** GO used to prepare FGS, GO-2, was prepared by the Staudenmaier method.<sup>9,16,19</sup> Elemental analysis showed that the GO composition was C<sub>10</sub>O<sub>3.68</sub>H<sub>2.48</sub>.

To make FGS, dried GO was charged into a quartz tube and flushed with argon for 10 min. The quartz tube was quickly inserted into a furnace preheated to 1,100 °C for 5 min to split the GO into individual sheets by the pressure resulted from CO<sub>2</sub> evolved by the thermal decomposition of functional groups.<sup>3-5,9</sup> The apparent specific volume was 410 cm<sup>3</sup>/g, and elemental analysis showed that the FGS composition was C<sub>10</sub>O<sub>0.51</sub>H<sub>0.50</sub>. The FGS had no visible peak by wide angle X-ray diffraction at  $2\theta>2^\circ$ .

**FGS/PMMA Nanocomposite Preparation.** MMA was polymerized under an N<sub>2</sub> atmospheric at 65 °C for 12 h while stirring with a magnetic bar to make nanocomposites in the presence of FGS and GO-1 with AIBN as an initiator. The recipes to prepare FGS/PMMA nanocomposites are shown in Table I. The sample designation code in Table I gives information about the amount of FGS and GO-1 included in each nanocomposite. For example, NC302 contains 3 parts FGS and 2 parts GO-1 per 100 parts MMA.

\*Corresponding Author. E-mail: hmjeong@mail.ulsan.ac.kr

**Table I. Recipes for the Preparing FGS/GO-1/PMMA Nanocomposites and Polymerization Yields**

Sample	Feed (by weight)					Polymerization Yield (%)
	MMA	FGS	GO-1	THF	AIBN	
NC000	100	-	-	-	0.3	94.2
NC050	100	0.5	-	-	0.3	92.7
NC100	100	1	-	-	0.3	92.1
NC101	100	1	1	-	0.3	89.7
NC300	100	3	-	150	0.3	90.3
NC301	100	3	1	200	0.3	90.2
NC302	100	3	2	200	0.3	89.5
NC303	100	3	3	200	0.3	90.6
NC500	100	5	-	400	0.3	89.3

THF was used as a diluent because low molecular weight liquid materials, such as MMA or THF, were required to obtain the required fluidity for mixing. Prepared FGS/PMMA nanocomposites were crushed into powder and dried at 65 °C under vacuum for 24 h to remove low molecular weight components.

**Measurements.** Direct current conductivity at room temperature was measured with a picoamperometer (Keithley 237) across a 1 mm thick film which was compression molded at 190 °C with a pressure of 22 MPa. The round silver electrodes measuring 0.28 cm<sup>2</sup> were attached at both surfaces of the specimen. Silver paste was used to ensure good contact between the specimen surface and the electrode.

The nanocomposite morphologies were examined by transmission electron microscopy (TEM, Hitachi H-8100). To prepare samples for TEM observation, the nanocomposite was pulverized. The nanocomposite powder was mixed with epoxy resin and cured at 70 °C for 24 h in a vacuum. The cured material was microtomed into slices and placed on a 200 mesh copper net. The TEM acceleration voltage was 200 kV.

Dynamic mechanical properties were determined using a dynamic mechanical analyzer (DMA, TA Instrument, DMA-Q800) in bending mode at a heating rate of 5 °C/min and 1 Hz. Samples were compression molded at 190 °C with a pressure of 22 MPa.

Differential scanning calorimetry (DSC) was carried out with a DSC 823<sup>e</sup> (Mettler Toledo) at a heating and cooling rate of 10 °C/min with 7 mg of sample. The samples stayed at 150 °C for 1 min in the DSC and were cooled to 25 °C. The glass transition temperature ( $T_g$ ) was measured in a subsequent heating scan.

## Results and Discussion

**Conductivity.** Table II shows that PMMA conductivity

**Table II. Physical and Thermal Properties of FGS/GO-1/PMMA Nanocomposites**

Sample	Conductivity (S/cm)	$E'$ (MPa)		$T_g$ (°C)	
		40 °C	170 °C	DSC	DMA
NC000	less than $10^{-14}$	1602	2.12	105.3	120.8
NC050	$2.46 \times 10^{-12}$	-	-	124.8	-
NC100	$1.89 \times 10^{-7}$	-	-	124.6	-
NC101	$2.50 \times 10^{-5}$	-	-	124.7	-
NC300	$5.17 \times 10^{-3}$	1781	7.83	124.4	133.7
NC301	$2.25 \times 10^{-2}$	1899	8.29	124.1	136.5
NC302	$2.11 \times 10^{-3}$	2152	12.13	125.3	135.0
NC303	$1.56 \times 10^{-3}$	2402	12.73	126.1	137.0
NC500	$4.89 \times 10^{-2}$	-	-	124.0	-

can be drastically improved by adding FGS. That is, the nanocomposite conductivities were improved more than  $10^7$ -fold by the presence of 1 part FGS and more than  $10^{11}$ -fold by 3 parts FGS compared to the pristine PMMA. These data show that the percolation threshold concentration is less than 1 wt% because FGS is finely dispersed in the PMMA matrix to effectively create conducting channels. A study of FGS/silicone foam nanocomposites by R. Verdejo *et al.* is the only open paper reporting on an FGS/polymer nanocomposite; however, no conductivity data is reported.<sup>14</sup> According to K. I. Winey *et al.*, SWCNT/PMMA nanocomposites prepared by coagulation to provide uniform dispersion and in which SWCNT has isotropic alignment have conductivities of about  $10^{-6}$  and  $10^{-3}$  S/cm when the SWCNT content is 1 and 3 wt%, respectively.<sup>20,21</sup> These results are comparable to the FGS/PMMA nanocomposites shown in Table II, suggesting that FGS is a good conducting filler that can substitute for SWCNT in various applications.

One can see in Table II that the NC101 conductivity is about 100-fold better than NC100, resulting from 1 part GO-1. Similarly, the NC301 conductivity is enhanced about 10-fold compared to NC300, resulting from 1 part GO-1. The NC301 conductivity is comparable to that of NC500. These results suggest that GO-1 has a compatibilizing effect, dispersing FGS in the PMMA matrix, with a consequent improvement in nanocomposite conductivity. This compatibilizing effect seems to be due to the facts that the structure of GO-1 is similar to FGS and GO-1 has polar functional groups that can interact with PMMA.

**TEM.** The TEM images of Figure 1 show that FGS is not randomly dispersed but oriented to a direction. This suggests that FGS can be easily oriented parallel to the top and bottom faces of the sample when compression molded, because FGS has one-atom thickness and high aspect ratio larger than 250~1,000.<sup>9</sup> The TEM image of NC300 (Figure 1(a)) shows single FGS and stacks of FGS which are finely

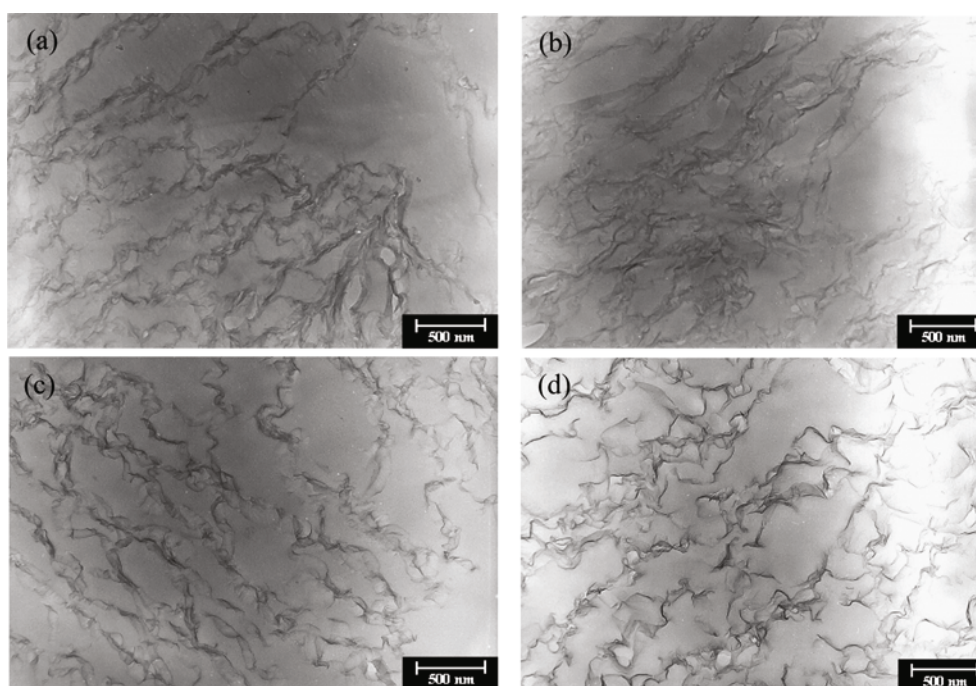


**Figure 1.** TEM micrographs of FGS/GO-1/PMMA nanocomposites: (a) NC300, (b) NC301, (c) NC302 and (d) NC303.

dispersed in the PMMA matrix with a wrinkled or hair-like structure, creating nanometer-scale conducting channels. In Figure 1(b), one can see that the channels are more diffuse than in Figure 1(a). This shows that GO-1 has a compatibilizing effect, improving FGS dispersion in the PMMA matrix resulting in enhanced conductivity. However, Figures 1(c) and 1(d) show that the FGS conducting channels become thinner and more distinct as the GO-1 content increases. This suggests that excess GO-1 reduces the broad FGS diffusion. The conductivities of the nanocomposites are ranked as follows: NC300 < NC301 > NC302 > NC303 (Table II). This result shows that although 1 part GO-1 can improve FGS dispersion, GO-1 can have adverse effects on FGS dispersion in a PMMA matrix at higher levels. This seems to be due to the facts that GO-1 is thicker than FGS because it is not exfoliated material, and the conductivity of GO-1 is lower than that of FGS.

**Mechanical and Thermal Properties of the FGS/GO-1/PMMA Nanocomposites.** The tensile storage modulus,  $E'$  at 40 °C and 170 °C, and  $\tan \delta$  peak temperature, i.e. the  $T_g$  measured by DMA, are summarized in Table II. These results show that the  $E'$ 's of NC300 are higher than that of a pristine sample, NC000, and these values increase further with additional GO-1 modification. These results demonstrate that FGS and GO-1 effectively reinforce the matrix PMMA. It has been reported that the  $E'$  of PMMA at 40 °C can be improved by more than 50% if reinforced with 1% carbon nanotube.<sup>22</sup> Table II shows that the  $E'$  increase of NC300 at 40 °C is 11% compared to NC000, which indicates that the reinforcing effect of FGS or GO-1 is weaker

than that of carbon nanotubes.

Table II shows that only 0.5 part FGS increases the  $T_g$  of NC010, measured by DSC, by about 20 °C. This shows that the PMMA chain mobility is effectively restricted in the presence of FGS. However, in Table II, it was almost same  $T_g$  in the 3~5% loaded FGS or GO-1/PMMA nanocomposites by DSC or DMA analysis. Further study is necessary to explain this lack of variation.

## Conclusions

Our results show that FGS is an effective conducting filler comparable to SWCNT. An FGS/PMMA nanocomposite containing 1 part FGS has a conductivity of  $1.89 \times 10^{-7}$  S/cm, more than  $10^7$ -fold better than pristine PMMA. This conductivity was enhanced a further 100-fold by addition of 1 part GO. Our results prove that GO is a good compatibilizer that can improve FGS dispersion in a PMMA matrix and consequently enhance nanocomposite conductivity, because GO has a structure chemically similar to FGS as well as polar functional groups that can interact with matrix PMMA molecules. Excess GO, however, has an adverse effect on conductivity.

FGS and GO also had a reinforcing effect. The  $E'$  of PMMA was increased by adding FGS and GO, and this effect was more evident at temperatures above  $T_g$ .

As little as 0.5 part FGS increased the  $T_g$  by about 20 °C from that of pristine PMMA, which demonstrates that FGS improves the thermal resistance of PMMA efficiently.

**Acknowledgements.** This work was supported by University of Ulsan Research Fund of 2007.

## References

- (1) B. Z. Jang, US Patent 0216222 (2006).
- (2) H.-K. Jeong, Y. P. Lee, R. J. W. E. Lahaye, M.-H. Park, K. H. An, I. J. Kim, C.-W. Yang, C. Y. Park, R. S. Ruoff, and Y. H. Lee, *J. Am. Chem. Soc.*, **130**, 1362 (2008).
- (3) H. C. Schniepp, J.-L. Li, M. J. McAllister, H. Sai, M. Herrera-Alonso, D. H. Adamson, R. K. Prud'homme, R. Car, D. A. Saville, and I. A. Aksay, *J. Phys. Chem. B*, **110**, 8535 (2006).
- (4) M. J. McAllister, J. L. Li, D. H. Adamson, H. C. Schniepp, A. A. Abdala, J. Liu, M. Herrera-Alonso, D. L. Milius, R. Car, R. K. Prud'homme, and I. A. Aksay, *Chem. Mater.*, **19**, 4396 (2007).
- (5) K. N. Kudín, B. Ozbas, H. C. Schniepp, R. K. Prud'homme, I. A. Aksay, and R. Car, *Nano Lett.*, **8**, 36 (2008).
- (6) T. Szabó, O. Berkesi, P. Forgó, K. Josepovits, Y. Sanakis, D. Petridis, and I. Dékány, *Chem. Mater.*, **18**, 2740 (2006).
- (7) A. B. Bourlinos, D. Gournis, D. Petridis, T. Szabó, A. Szeri, and I. Dékány, *Langmuir*, **19**, 6050 (2003).
- (8) A. Lerf, H. He, M. Forster, and J. Klinowski, *J. Phys. Chem. B*, **102**, 4477 (1998).
- (9) R. K. Prud'Homme, I. A. Aksay, D. Adamson, and A. Abdala, US Patent 0092432 (2007).
- (10) S. H. Lee, J. S. Park, C. M. Koo, B. K. Lim, and S. O. Kim, *Macromol. Res.*, **16**, 261 (2008).
- (11) B.-S. Kim, K.-D. Suh, and B. Kim, *Macromol. Res.*, **16**, 76 (2008).
- (12) I. Park, M. Park, J. Kim, H. Lee, and M. S. Lee, *Macromol. Res.*, **15**, 498 (2007).
- (13) W. K. Park, J. H. Kim, S.-S. Lee, J. Kim, G.-W. Lee, and M. Park, *Macromol. Res.*, **13**, 206 (2005).
- (14) R. Verdejo, F. Barroso-Bujans, M. A. Rodriguez-Perez, J. A. de Saja, and M. A. Lopez-Manchado, *J. Mater. Chem.*, **18**, 2221 (2008).
- (15) J. Y. Jang, M. S. Kim, H. M. Jeong, and C. M. Shin, *Compos. Sci. Technol.*, **69**, 186 (2009).
- (16) N. D. Anh, Y. R. Lee, A. V. Raghu, H. M. Jeong, C. M. Shin, and B. K. Kim, *Polym. Int.*, **58**, 412 (2009).
- (17) W. Wen-Ping and P. Cai-Yuan, *Polym. Eng. Sci.*, **44**, 2335 (2004).
- (18) R. Bissessur, P. K. Y. Liu, and S. F. Scully, *Synthetic Metals*, **156**, 1023 (2006).
- (19) C. Hontoria-Lucas, A. J. López-Peinado, J. López-González, M. L. Rojas-Cervantes, and R. M. Martín-Aranda, *Carbon*, **33**, 1585 (1995).
- (20) F. Du, J. E. Fischer, and K. I. Winey, *Phys. Rev. B*, **72**, 121404(R) (2005).
- (21) F. Du, R. C. Scogna, W. Zhou, S. Brand, J. E. Fischer, and K. I. Winey, *Macromolecules*, **37**, 9048 (2004).
- (22) C. Velasco-Santos, A. L. Martínez-Hernández, F. T. Fisher, R. Ruoff, and V. M. Castaño, *Chem. Mater.*, **15**, 4470 (2003).